

## Remote Sensing Signatures of Breaking Waves from Multi-Instrument Field Experiment on FLIP

M.D. Anguelova,<sup>1</sup> D.J. Dowgiallo,<sup>1</sup> G.B. Smith,<sup>1</sup>  
S.L. Means,<sup>2</sup> I.B. Savelyev,<sup>1</sup> G.M. Frick,<sup>1</sup> C.M. Snow,<sup>1</sup>  
J.A. Schindall,<sup>2</sup> and J.P. Bobak<sup>1</sup>

<sup>1</sup>Remote Sensing Division

<sup>2</sup>Acoustics Division

**Introduction:** Oceanic whitecaps are the surface expression of breaking wind waves in the ocean. Whitecap fraction  $W$ , defined as the fraction of a unit surface covered with sea foam, quantifies wave breaking and is thus a suitable forcing variable for parameterizing and predicting air-sea interaction processes associated with breaking waves. Whitecaps in different lifetime stages have markedly different properties. Active whitecaps, formed at the moment of active breaking, are thick, comprise a wide range of bubble sizes, move along with the wave crest, and cover less surface area. Residual whitecaps, comprising decaying foam, are thinner, remain motionless behind the wave that has created them, and spread over a larger area. Total  $W$  (active plus residual whitecaps) is a useful predictor of bubble-mediated sea spray production and heat exchange.<sup>1</sup> More dynamical air-sea processes are better represented by active whitecap fraction  $W_A$ , e.g., production of spume droplets (important for tropical storms intensification), momentum flux, turbulent mixing, gas exchange, and generation of ambient noise in the ocean.<sup>2</sup>

A database of  $W$  from satellite-measured brightness temperature  $T_B$  of the ocean surface at microwave frequencies has been developed within the framework of the WindSat mission at NRL.<sup>3</sup> This database is useful for studying and parameterizing  $W$  variability. However, to make this database useful for dynamic processes, it is necessary to find a way to extract  $W_A$  from  $W$ . We pursue separation of  $W_A$  from  $W$  both theoretically and experimentally. The physical basis for the experimental approach is that there are distinct signature differences between active and residual whitecaps at infrared (IR) wavelengths.<sup>4</sup> To this end, we conducted a multi-instrument field campaign to collect data useful for identifying the signatures of breaking waves and whitecaps at different electromagnetic wavelengths, from visible, to IR, to microwave.

**Field Campaign:** We collected data from April 22 to 30, 2012, on the Floating Instrument Platform (FLIP) drifting along the coast of California from Monterey Bay south. FLIP is a unique vessel (<http://www-mpl.ucsd.edu/resources/flip.intro.html>) that provides a stable research platform for data collection on three

booms (port, starboard, and face). FLIP is towed to its operating area in a horizontal position and, through ballast changes, is “flipped” to a vertical position to become a stable spar buoy with a draft of 300 ft (Fig. 3(a)). The diameter of the hull tapers with depth, and this makes FLIP less responsive to wave motion.

Variations of ocean surface brightness temperature,  $T_B$ , caused by breaking waves and whitecaps were measured with microwave radiometers at frequencies of 10 and 37 GHz, vertical and horizontal (VH) polarizations. The radiometers, mounted on the port boom within a weather casing (Fig. 3(b)), looked at the ocean surface at an angle of 45°. The beamwidths of the 10- and 37-GHz horns are approximately 6°, giving an approximate footprint of 1.8 m in diameter for each instrument. The infrared imager used during this exercise was a Merlin-Mid (Indigo Systems, a division of FLIR). This system is sensitive to radiation in the 3 to 5  $\mu\text{m}$  band (mid-wave infrared) and has a noise equivalent  $\Delta T$  of approximately 0.017 K. Imagery was typically collected at a sampling rate of 10 Hz. The IR camera was mounted on top of the radiometers (Fig. 3(b)) to ensure the radiometer footprints fell within the

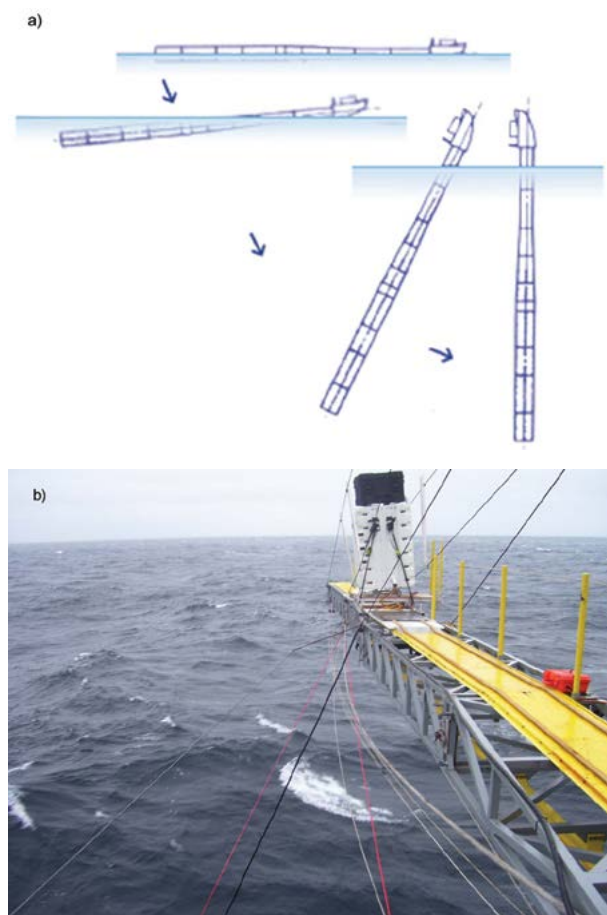


**FIGURE 3** Research platform FLIP: a) controlled sinking to vertical position; b) instrumentation deployed on port boom.

16 × 12 m<sup>2</sup> field of view (FOV) of the IR camera. Three video cameras, positioned in different places, recorded visible images of whitecaps.

An acoustic vertical line array (VLA) provided data for the bubble-generated noise beneath breaking waves. The VLA was suspended between the face and port booms of FLIP. The array consisted of three nested apertures with hydrophones spaced at 1.25, 0.625, and 0.3125 m, yielding design frequencies of 600, 1200, and 2400 Hz, respectively. The VLA was deployed at a depth such that the upward endfire beam would isolate acoustic signatures from individual breaking waves, excluding FLIP-generated noise at all but the lowest frequencies.

The aerosol size distribution was measured with two instruments. A Particle Measuring Systems CSASP-100-HV, suspended from the starboard boom, measured aerosol from 0.25 to 23.5 μm radius. The NRL Differential Mobility Analyzer measured ducted and dried aerosol between 6 and 400 nm radii.

Various auxiliary data such as wind speed, air temperature, humidity, wave field, and water temperature profile characterize the experimental conditions. The conditions encountered ranged from wind speed of 2.8 to about 18 m s<sup>-1</sup>, and significant wave height from 1 to ~5 m (Fig. 4).

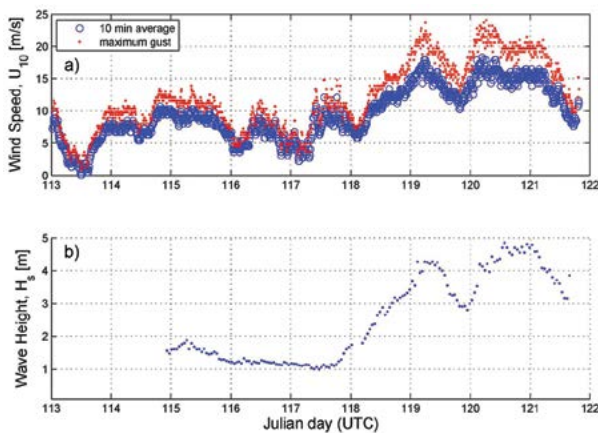


**FIGURE 4**  
Experimental conditions: a) wind speed; b) significant wave height.

**Data Collected:** Figure 5 shows typical data collected from each instrument. A bright whitecap seen in the visible image (Fig. 5(a)) is identified by dark streaks at IR wavelengths (Fig. 5(b)). Spikes in  $T_b$  at 10 GHz, seen simultaneously in both H and V polarizations, mark whitecap signatures at microwave wavelengths (Fig. 5(c)). The observed increased noise level (in dB) is the whitecap acoustic signature (Fig. 5(d)).

IR images will help us identify active and residual foam as warm and cold patches, respectively. Matching these signals in time with radiometric, acoustic,

and aerosol data will help us identify the signatures of the two life stages at other wavelengths. We will then establish criteria for active vs residual separation for each type of data. Correlating radiometric, acoustic, and aerosol signature characteristics with each other, as well as with meteorological and oceanographic data, will yield empirical relationships useful for predicting breaking wave and whitecaps with observations from various sensors.

The impact of our findings will be the improvement of the current accuracy of predicting air-sea fluxes at the air-sea interface. More accurate air-sea fluxes will, in turn, reduce the uncertainty of weather forecasting, tropical cyclone intensification, wave forecasting, and climate prediction.

**Acknowledgments:** This work was sponsored by the Office of Naval Research (ONR), NRL Program element 61153N WU 4500. We highly appreciate the funding support for our use of FLIP by Robert Schnoor via the Naval Research Facilities Program at ONR, and by Dr. Joan Gardner and Dr. Edward Franchi via the NRL Platform Support Program. Captain William Gaines, FLIP program manager at Marine Physics Laboratory (MPL) at Scripps Institution of Oceanography, was indispensable in organizing the field campaign. We appreciate Tom Golfinos, Officer-in-Charge for FLIP, and crew members Johnny, Dave, Frank, and Jerry for their hard work, endurance, and camaraderie. We would also like to thank George Trekas and his colleagues at the MPL Machine Shop for their expertise and skills in devising the instrument deployment on the FLIP booms.

[Sponsored by ONR]

#### References

- <sup>1</sup> G. de Leeuw, E. Andreas, M.D. Angelova, C. Fairall, E. Lewis, C. O'Dowd, M. Schulz, and S. Schwartz, "Production Flux of Sea-Spray Aerosol," *Rev. Geophys.* **49** (2011).
- <sup>2</sup> W.K. Melville, "The Role of Surface-Wave Breaking in Air-Sea Interaction," *Annu. Rev. Fluid Mech.* **28**, 279–321 (1996).
- <sup>3</sup> P.W. Gaiser, K.M. St Germain, E.M. Twarog, G.A. Poe, W. Purdy, D. Richardson, W. Grossman, W.L. Jones, D. Spencer, G. Golba, J. Cleveland, L. Choy, R.M. Bevilacqua, and P.S. Chang, "The WindSat Spaceborne Polarimetric Microwave Radiometer: Sensor Description and Early Orbit Performance," *IEEE Trans. Geosci. Rem. Sens.* **42**, 2347–2361 (2004).
- <sup>4</sup> G.O. Marmorino and G.B. Smith, "Bright and Dark Ocean Whitecaps Observed in the Infrared," *Geophys. Res. Lett.* **32**, L11604 (2005).

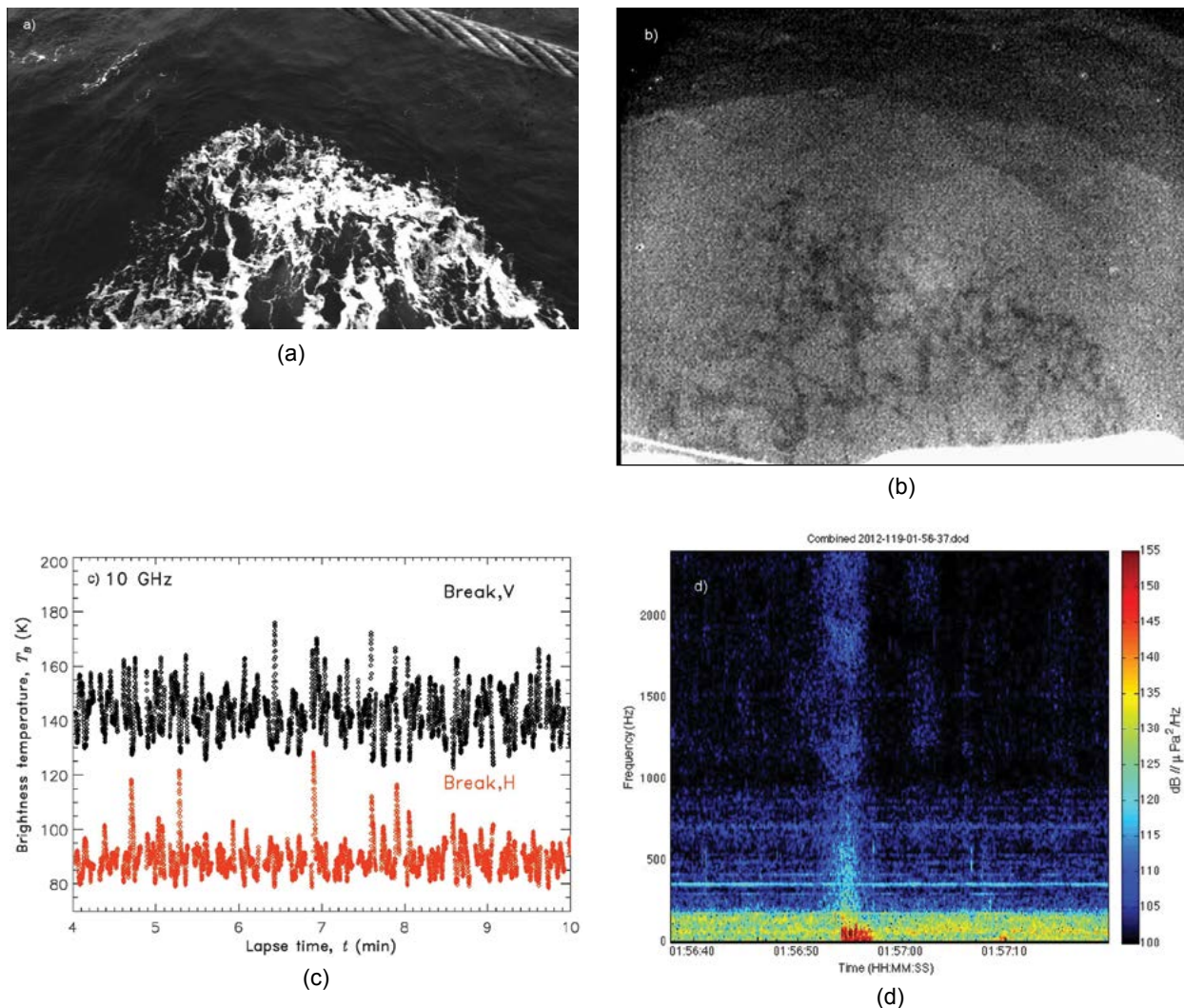


**FIGURE 5** Breaking wave signatures at different wavelengths: a) visible; b) infrared; c) microwave (10 GHz); and d) acoustic.

## Surprising Discoveries in Reflectance Properties of Complex Granular Sediments

A. Abelev<sup>1</sup> and C.M. Bachmann<sup>2</sup>

<sup>1</sup>Marine Geosciences Division

<sup>2</sup>Remote Sensing Division

**Introduction and Background:** Terrestrial remote sensing applications are abundant in various fields of science and technology, applicable and currently in high demand in both the civilian and the military domains. One of the main goals of these applications is determination of the nature, properties, and composition of soils — natural and engineered alike. Multi- and hyperspectral measurements represent one of the main and quickly growing sectors of remote sensing, with

sensors deployed near the ground, in the air, and in Earth's orbit. The characteristic nature of the way that these sensors are used involves a phase angle dependence of measurements (angle between the line of sensor sight and the illumination line of the sun). This influence is expressed in models via a bidirectional reflectance distribution function (BRDF). Characteristics such as texture, grain-size distribution, and mineralogical composition are phase-angle dependent and represent the first level of complexity in characterizing soil properties and behaviors. These properties are features of the very surface of the soil, visible on the scale of the wavelength of a hyperspectral instrument spectrum, typically including some parts or all of the visible (VIS), near infrared (NIR), and shortwave IR (SWIR) ranges (0.4 to 2.5  $\mu\text{m}$ ). Additionally, some of the bulk properties of the soils are of great interest to the end-user and include, e.g., bulk density and porosity. Describing these properties involves the mechani-